



## ORIGINAL ARTICLE

# Experimental study and development of mathematical model using surface response method to predict the rheological performance of CeO<sub>2</sub>-CuO/10W40 hybrid nanolubricant



Mojtaba Sepehrnia <sup>a,b,\*</sup>, Mohammad Javad Farrokh <sup>b</sup>, Mahsa Karimi <sup>c</sup>,  
Kazem Mohammadzadeh <sup>d,\*</sup>

<sup>a</sup> Department of Mechanical Engineering, Technical and Vocational University, Qom, Iran

<sup>b</sup> Department of Mechanical Engineering, Shahabdanesh University, Qom, Iran

<sup>c</sup> Faculty of Mechanical Engineering, University of Kashan, Kashan, Iran

<sup>d</sup> Department of Mechanical Engineering, Arak University of Technology, Arak, Iran

Received 2 October 2022; accepted 21 February 2023

Available online 27 February 2023

## KEYWORDS

Dynamic viscosity;  
Hybrid nano-lubricant;  
Experimental measurement;  
Cerium dioxide;  
Copper oxide;  
Response Surface Method

**Abstract** In this study, the rheological behavior of CeO<sub>2</sub>-CuO/10W40 hybrid nanolubricant with several volume fractions (VFs) over the range of 0.25–1.5 vol%, temperatures over the range of 5–55 °C, and shear rates varying from 20 to 1000 rpm are experimentally assessed. The viscosity measurements at various shear rates (SRs), VFs, and temperatures demonstrated that the 10W40 engine oil and hybrid nanolubricant behave non-Newtonian. The experimental results show that the maximum viscosity reduction with increasing SR occurs at T = 45 °C and VF = 1.25 %, which its value is about 30.28 %. The experimental findings demonstrate that an increase in temperature results in reduced viscosity (between 91.84 % and 93.10 %) while the viscosity increases with increasing VF. To forecast the experimental data, two correlations (functions of three variables: temperature, VF, and SR) are presented based on experimental data using curve fitting and the response surface method (RSM). The results show that good concordance exists between experimental data and correlation results to estimate the viscosity of CeO<sub>2</sub>-CuO/10W40 hybrid nano-lubricant. Additionally, the correlation developed by the RSM is more straightforward than one derived from curve fitting. This new hybrid nano-lubricant can be used as a coolant in the automotive industry.

© 2023 The Author(s). Published by Elsevier B.V. on behalf of King Saud University. This is an open access article under the CC BY-NC-ND license (<http://creativecommons.org/licenses/by-nc-nd/4.0/>).

\* Corresponding authors.

E-mail addresses: [m.sepehrnia@shdu.ac.ir](mailto:m.sepehrnia@shdu.ac.ir) (M. Sepehrnia), [k.mohammadzadeh@arakut.ac.ir](mailto:k.mohammadzadeh@arakut.ac.ir) (K. Mohammadzadeh).

Peer review under responsibility of King Saud University.



## 1. Introduction

Hybrid nanofluids have emerged as a new class of colloidal fluids that have attracted attention due to the potential adaptation of their thermophysical properties to improve heat transfer through a combination of more than one nanoparticle to address specific application requirements (Esfe et al., 2015; Asadi and Asadi, 2016; Dalkılıç, 2018; Ghaffarkhah et al., 2019). The rheological behavior of hybrid nanofluids has an important impact on the hydraulic and thermal resistances and thermal capacity of the fluid (Huminić and Huminić, 2018). The complex behaviors and characteristics of hybrid nanofluids have led most research in this field to experimental work. The rheological analysis of hybrid nanofluids is necessary, taking into account the effect of the nanoparticles volume fraction (VF), temperature (T), shear stress (SS), and shear rate (SR) on the viscosity of the hybrid nanofluids and investigated in several studies (Esfe et al., 2022; Mokarian and Ameri, 2022; Cao et al., 2021; Giwa et al., 2021; Barkhordar et al., 2021; Asadi et al., 2021; Asadi et al., 2021; Sepehrnia et al., 2022). During the past decade, surveys were conducted to ascertain the dynamic viscosity of hybrid nano-lubricant. In the literature on hybrid nanofluids, hybrid nanofluids containing nanoparticles of cerium oxide ( $\text{CeO}_2$ ) and copper oxide ( $\text{CuO}$ ) have been less studied, which are reviewed in this section.

The rheological behavior of  $\text{CeO}_2$ - $\text{CuO}$ /coconut oil hybrid nanolubricants are experimentally and theoretically examined in various weight fractions (wt%) over the range 0% to 1% for different mixture ratios of  $\text{CeO}_2$  and  $\text{CuO}$ , namely 25/75, 50/50, and 75/25 at the temperature of 30–90 °C and various SRs by Sajeeb and Rajendrakumar (Sajeeb and Rajendrakumar, 2019). They observed non-Newtonian behavior for higher concentrations and lesser SRs for each mixture ratio of  $\text{CeO}_2$  and  $\text{CuO}$ . But at higher SRs, Newtonian behaviors are observed at all temperatures and concentrations. Sepehrnia et al. (Sepehrnia et al., 2022) studied the rheological properties of the  $\text{CeO}_2$ - $\text{SnO}_2$ /SAE50 hybrid nanofluid at different temperatures of 25–67 °C, as well as VFs of 0.25–1.5%, and the SRs of 1333–2932.6  $\text{s}^{-1}$ . The results demonstrated that the investigated hybrid nanofluid is a non-Newtonian fluid. Their results showed that the maximum dynamic viscosity occurs at a VF of 1.5%, and a temperature of 25 °C. Sajeeb and Rajendrakumar (Sajeeb and Rajendrakumar, 2020) studied the tribological performance of a new  $\text{CeO}_2$ - $\text{CuO}$ /coconut oil hybrid nanolubricant in different mixture ratios of  $\text{CeO}_2$ / $\text{CuO}$  (25/75, 50/50, and 75/25) at different concentrations of 0.1 to 1.0 wt%. A decrease of 15.7% in average friction factor was detected using 0.25 wt%  $\text{CeO}_2$ / $\text{CuO}$  (50/50). Sepehrnia et al. (Sepehrnia et al., 2022) analyzed the viscosity of  $\text{CeO}_2$ -GO-SA/10W40 ternary hybrid nanofluid over the VF range restricted to 1.5% and over the temperature range of 5–55 °C. Their results showed that the maximum dynamic viscosity occurs at a temperature of 5 °C, and a VF of 1.5%. Also, rheological probations showed that fabricated ternary hybrid nanofluid is non-Newtonian.

The dynamic viscosity measurement of  $\text{CuO}$ -MWCNTs (50–50%)/SAE 5w–50 hybrid nanofluid is performed by Aghaei et al. (Aghaei et al., 2018) over the range of 0.05% < VFs < 1%, at temperatures of 5 to 55 °C. Experimental findings show that the viscosity increases by increasing VF and reduces by increasing temperature, and nanofluid behaves like a Newtonian fluid. They predicted the hybrid nanofluid viscosity using an ANN model and established a novel viscosity model. Abdollahi Moghaddam et al. (Moghaddam and Motahari, 2017) experimentally investigated the rheological behavior of  $\text{CuO}$ -MWCNTs (70–30%)/SAE40 hybrid nanofluid over the range 0.0625% < VFs < 1% and temperature of 20 °C to 50 °C. They found that  $\text{CuO}$ -MWCNTs/SAE40 hybrid nanofluid is non-Newtonian. Esfe et al. (Esfe et al., 2018) experimentally investigated the viscosity of low concentration  $\text{CuO}$ -MWCNTs (90–10%)/10w40 hybrid nanofluid in different VFs (0.01%, 0.1%, 0.25%, 0.5%, 0.75%, and 1%). They discovered that when VF increases, the nanofluid viscosity also increases. Additionally, their rheological experiments showed that the fabricated hybrid nanofluid has a non-Newtonian behavior as like

pure oil (10w40). In another experimental study, Esfe et al. (Esfe et al., 2023) experimentally studied the viscosity of  $\text{CuO}$ -MWCNTs (60–40%)/10W40 hybrid nanofluid in the VF range of 0.5–1.0% at the temperatures of 5–55 °C. Their results of the experimental study reveal the non-Newtonian behavior of hybrid nanofluid. Esfe et al. (Esfe et al., 2019) experimentally examined the rheological performance of  $\text{CuO}$ -MWCNTs (70–30%)/SAE50 hybrid nanofluid over the range 0% < VFs < 1%, at temperatures of 25–50 °C and the SRs of 666–7998  $\text{s}^{-1}$ . They found that nanofluid can behave similarly to non-Newtonian fluids. In addition, a mathematical relationship for the relative viscosity of hybrid nanofluid is developed, and the relative viscosity sensitivity to temperature and VF is performed. In a laboratory study on the ternary hybrid nanofluid, Mansourian et al. (Mansourian et al., 2021) examined the rheological properties of  $\text{CuO}$ - $\text{SiO}_2$ - $\text{CaP}$ /crude oil ternary hybrid nanofluid in the VF range of 0.05–0.75% at temperatures of 25–55 °C. The results proved that the base fluid behaves Newtonian. Newtonian performance was also detected for the nanofluid with VFs up to 0.75%.

By reviewing the experimental studies performed by researchers, it is found that the rheological performance of hybrid nanolubricants containing  $\text{CeO}_2$  is less studied, and there is a need for further study. Therefore, in the present experimental work, the rheological performance of  $\text{CeO}_2$ - $\text{CuO}$ /10W40 hybrid nanolubricant with a temperature ranging from 5 °C to 55 °C, the VF ranging from 0.25 to 1.5%, and the SR ranging from 20 to 1000 rpm is assessed. Additionally, two new three-variable correlations are developed based on experimental data using curve fitting and the response surface method (RSM) to precisely anticipate the dynamic viscosity of  $\text{CeO}_2$ - $\text{CuO}$ /10W40 hybrid nanolubricant. Furthermore, the sensitivity analysis of dynamic viscosity is performed.

## 2. Experiments

In the present study, the base fluid is 10W40 engine oil manufactured by Castrol company. Fig. 1 shows the base fluid and the nanoparticles of  $\text{CeO}_2$  and  $\text{CuO}$  (supplied by the US Research Nanomaterials, Inc.). The characteristics of nanoparticles are also presented in Fig. 1.

The material size and purity of nanoparticles are obtained via X-Ray Diffraction (XRD) results (Fig. 2). The pointed and thin peak in the XRD diagram indicates that both nanoparticles of  $\text{CeO}_2$  and  $\text{CuO}$  have perfect crystal phase structure. Moreover, impurity peaks are not observed at the detection limit of XRD, which shows that this technique is capable of generating  $\text{CeO}_2$  and  $\text{CuO}$  powders in a single phase.

### 2.1. Preparation of hybrid nanolubricant and measurement of dynamic viscosity

The  $\text{CeO}_2$ - $\text{CuO}$ /10W40 hybrid nanolubricant is prepared at different VFs of 0.25, 0.5, 0.75, 1.0, 1.25, and 1.5 %. The total nanoparticle VF ( $\phi$ ) in the hybrid nanolubricant is evaluated using Eq. (1).

$$\phi = \left( \frac{\left(\frac{M}{\rho}\right)_{\text{CeO}_2} + \left(\frac{M}{\rho}\right)_{\text{CuO}}}{\left(\frac{M}{\rho}\right)_{\text{oil}} + \left(\frac{M}{\rho}\right)_{\text{CeO}_2} + \left(\frac{M}{\rho}\right)_{\text{CuO}}} \right) \times 100 \quad (1)$$

Where,  $M$  represents the mass (kg), and  $\rho$  denotes the density ( $\text{kg}/\text{m}^3$ ). The mass measurement of  $\text{CeO}_2$  and  $\text{CuO}$  nanoparticles is performed through a weight scale with an accuracy of 1 mg. In brief, the two-step method and Brookfield viscometer are applied for the preparation and the viscosity

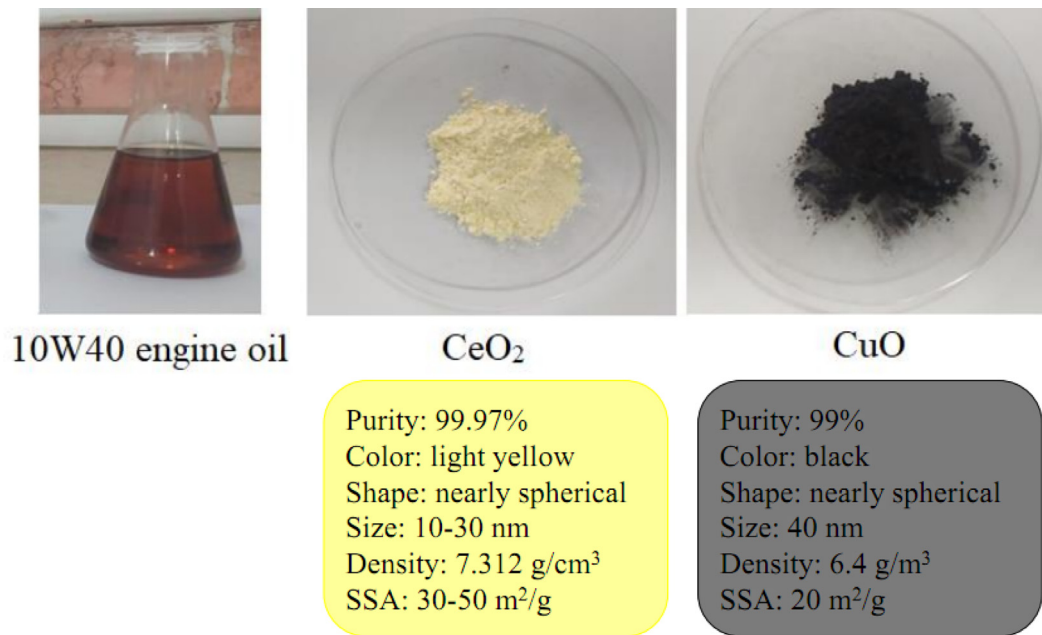


Fig. 1 Base fluid and the characteristics of the used nanoparticles.

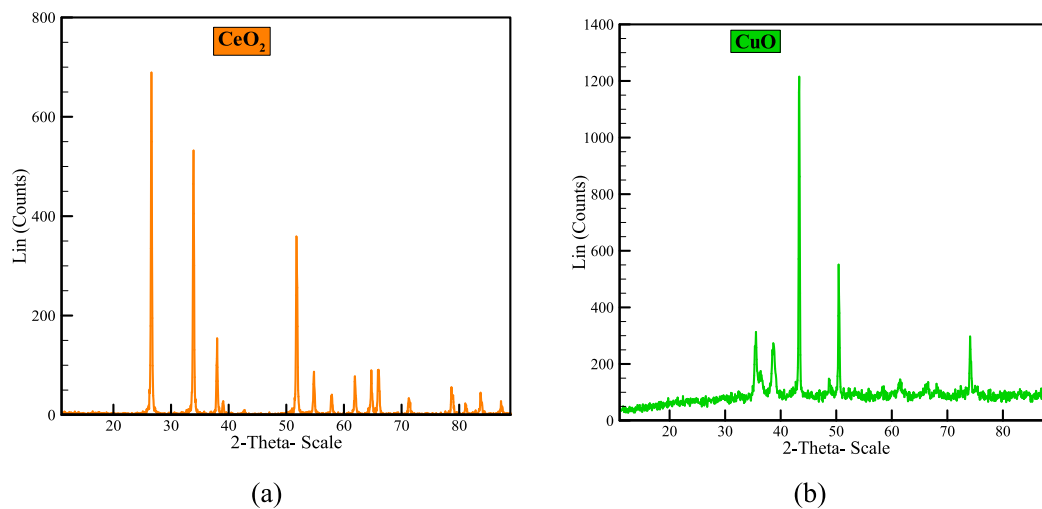


Fig. 2 XRD chart: (a) CeO<sub>2</sub> and (b) CuO.

measurement of hybrid nanolubricants, respectively. The necessary amounts of nanoparticles are dispersed in the base fluid to reach the desired VF. To prevent agglomeration of nanoparticles and perform the suspension process, nanofluids are rotated using a magnetic stirrer for 1 h and exposed to ultrasonic waves for 1.5 h.

The measurement of the nanolubricant sample viscosities with various VFs is accomplished in different nanolubricant temperatures of 5 – 55 °C, and SRs of 20–1000 rpm. Samples of nanolubricant are illustrated in Fig. 3. Additionally, after a month of preparation of nanofluids, no deposition or agglomeration was observed in the prepared samples and the stability of the samples was ensured.

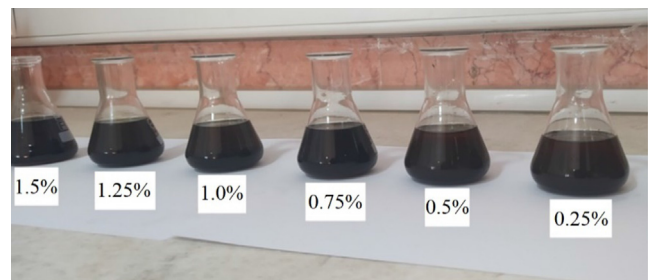


Fig. 3 Samples of prepared hybrid nanolubricants (after a month).

### 3. Results and discussion

#### 3.1. Rheological properties

Evaluating the rheological properties of hybrid nanolubricants is critical in fluid mechanics and heat transfer applications (Dalkılıç, 2018; Asadi et al., 2016; Afrand et al., 2016). To recognize how a nanofluid behaves Newtonian or non-Newtonian, its viscosity needs to be measured at various SRs (Sepehrnia et al.,

2022). The shear stress (SS) is plotted against SR for CeO<sub>2</sub>-CuO/10W40 hybrid nanolubricant at various VFs and temperatures, in Fig. 4. It is pretty clear that the increase in SR results in an increase in SS across all VFs. The hybrid nanolubricant SS decreases under high temperatures at constant SR due to the decrease of intermolecular forces of the hybrid nanolubricant. As shown in Fig. 4, the apparent dynamic viscosity of the hybrid nanolubricant (slope of the tangent line to the SS-SR curve) increases with decreasing temperature.

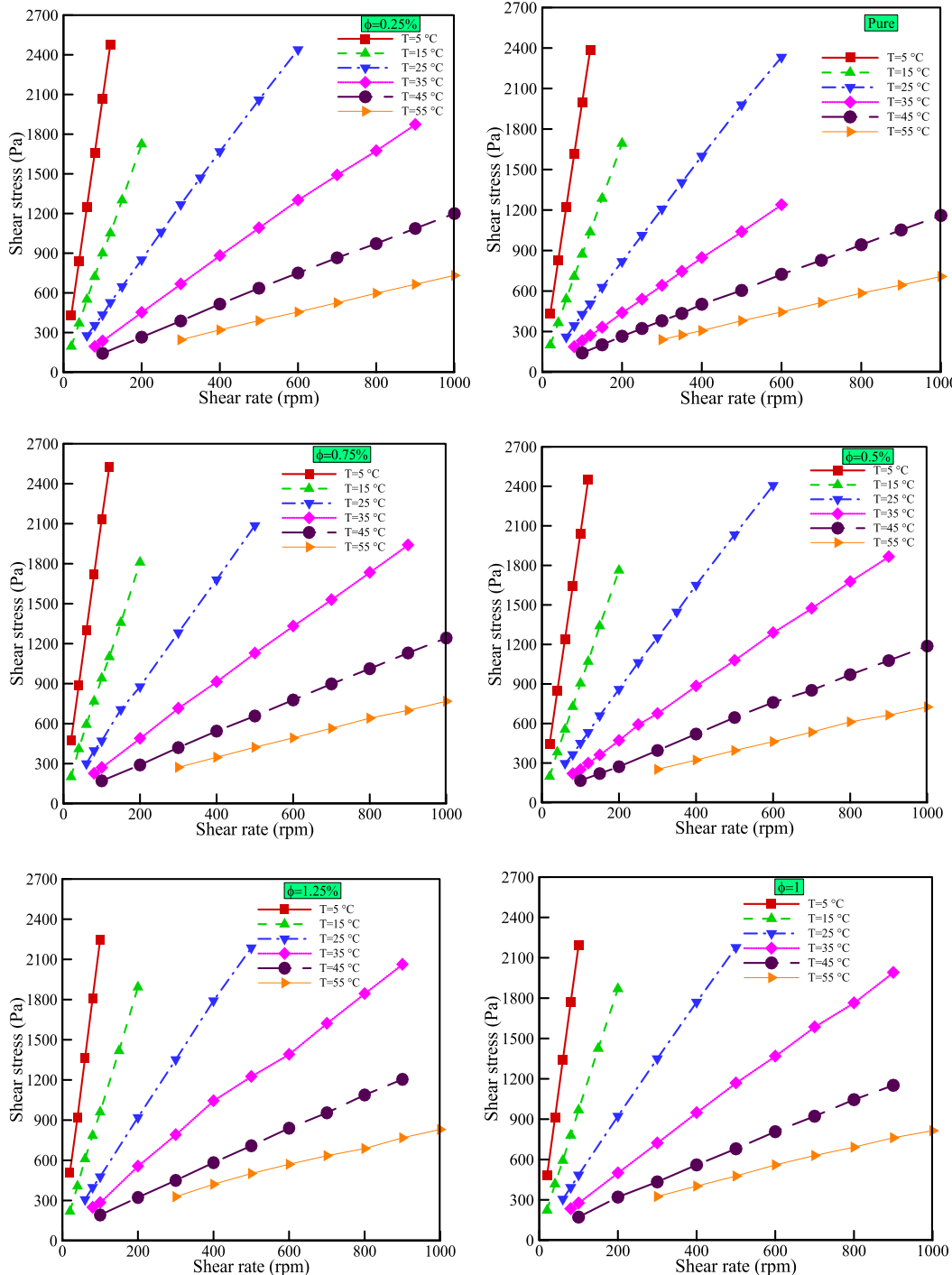


Fig. 4 SS versus SR at different temperatures and VFs.

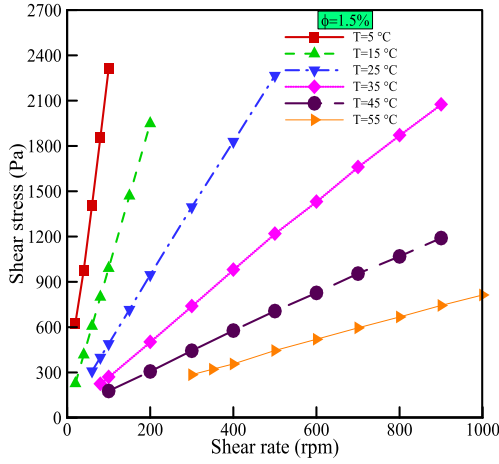


Fig. 4 (continued)

Changes in the viscosity of the hybrid nanofluid relative to SR at different VFs and temperatures are depicted in Fig. 5. The nonlinearity of the curves indicates the non-Newtonian property of the hybrid nanolubricant.

The quantitative results for the minimum and maximum percentages of viscosity reduction with the SR for different VFs and temperatures are summarized in Table 1. As shown in Table 1, the maximum viscosity reduction is achieved with hybrid nanofluid at VF and temperature of 1.25% and 45 °C, so by changing the SR from 100 to 900 rpm, the dynamic viscosity is reduced by 30.28%. Consequently, the hybrid nanolubricant under investigation acts as a pseudoplastic fluid at all temperatures and VFs. This behavior can be ascribed to heat production at elevated SRs. Moreover, it can be seen that the hybrid nanolubricant behavior deviates further from Newtonian behavior under low temperatures.

To ensure the non-Newtonian performance of CeO<sub>2</sub>-CuO/10W40 hybrid nanolubricant, the consistency and power-law indices ( $m$  and  $n$ ) of the familiar Ostwald de Waele relationship (Eq. (2)) are presented in Table 2 and Table 3, respectively.

$$\tau = m\dot{\gamma}^n \quad (2)$$

It can be understood from Table 2 that the  $m$  declines with increasing temperature from 5 to 55 °C, which is compatible with decreasing dynamic viscosity due to the temperature increase in Fig. 4. In addition,  $m$  values increase slightly from 45 to 55 °C at VFs of 1% and 1.25%, which indicates the prevention of a drastic reduction in dynamic viscosity with rising temperature. Additionally, based on Table 3,  $n$  is  $< 1$  for all temperatures and VFs, from which it can be inferred that the hybrid nanolubricant has the same properties as pseudoplastic fluid.

### 3.2. The effects of temperature and VF on nanolubricant dynamic viscosity

Awareness of changes in the lubricants dynamic viscosity with temperature is particularly important in the industry. The effect of temperature change on the hybrid nanolubricant dynamic viscosity with various VFs at SRs of 100 and 500 rpm is shown in Fig. 6. It is detected that increasing the

temperature reduces the hybrid nanolubricant viscosity. For example, with an SR of 100 rpm, the temperature change from 5 to 45 °C results in a 93.10% and 91.84% drop in dynamic viscosity at VFs of 0.25% and 0.5%, respectively. In fact, with increasing temperature, molecular motions increase, so cohesive forces are reduced with a corresponding reduction in resistance to motion. For high VFs, the temperature effect on dynamic viscosity change becomes more vigorous. This behavior can be ascribed to the more probable clustering of nanoparticles at high VFs.

The dynamic viscosity changes of CeO<sub>2</sub>-CuO/10W40 hybrid nanolubricant in terms of VF are represented in Fig. 7. in SRs of 100 and 500 rpm. As can be seen, the viscosity increases with increasing VF at all temperatures. For example, at an SR of 100 rpm and a temperature of 5 °C, with increasing VF, the viscosity increases by 15.6%, and this increase is 14.48% at an SR of 500 rpm and a temperature of 25 °C. This is because as the nanoparticles disperse into the base fluid, the interactions of the base fluid molecules and the nanoparticles are increased, which increases the fluid flow resistance and increases the dynamic viscosity. Furthermore, with increasing VF, more flow resistance is created as a result of increasing nanoparticle intermolecular forces.

### 3.3. Effect of temperature and VF on the relative viscosity

The effect of temperature and VF on the relative viscosity of CeO<sub>2</sub>-CuO/10W40 hybrid nano-lubricant ( $\mu_r = \mu_{nf}/\mu_{bf}$ ) is illustrated in Fig. 8. The increase in viscosity of the hybrid nanofluid compared to the base fluid can be observed at all temperatures and VFs, which was also observed in previous studies (Sepehrnia et al., 2022). Also, the results of Fig. 8 show that the maximum increase in hybrid nanofluid viscosity compared to the base fluid at a constant temperature is 35.85%, which is related to hybrid nanofluid with a VF of 1.25% and a temperature of 45 °C. In addition, the minimum increase in hybrid nanofluid viscosity compared to the base fluid is 0.94%, which is related to hybrid nanofluid with a VF of 0.25% and a temperature of 45 °C.

### 3.4. Proposed correlations

Several familiar correlations have been established to estimate nanofluid viscosity, such as the correlation of Einstein (Einstein, 1911), Brinkman (Brinkman, 1952), Batchelor (Batchelor, 1977), and Wang et al. (Wang and Mujumdar, 2007), which are given in Eqs (3) to (6), respectively.

$$\mu_r = 1 + 2.5\varphi \quad (3)$$

$$\mu_r = (1 - \varphi)^{-2.5} \quad (4)$$

$$\mu_r = 1 + 2.5\varphi + 6.2\varphi^2 \quad (5)$$

$$\mu_r = 1 + 7.3\varphi + 123\varphi^2 \quad (6)$$

The relative viscosity of CeO<sub>2</sub>-CuO/10W40 hybrid nanolubricant obtained from the experimental data of the present work is compared with the results predicted by the Eqs (3) to (6) at SR of 100 rpm in Fig. 9. Conventional models are temperature independent and show a linear behavior, while the results of the present study are completely temperature-

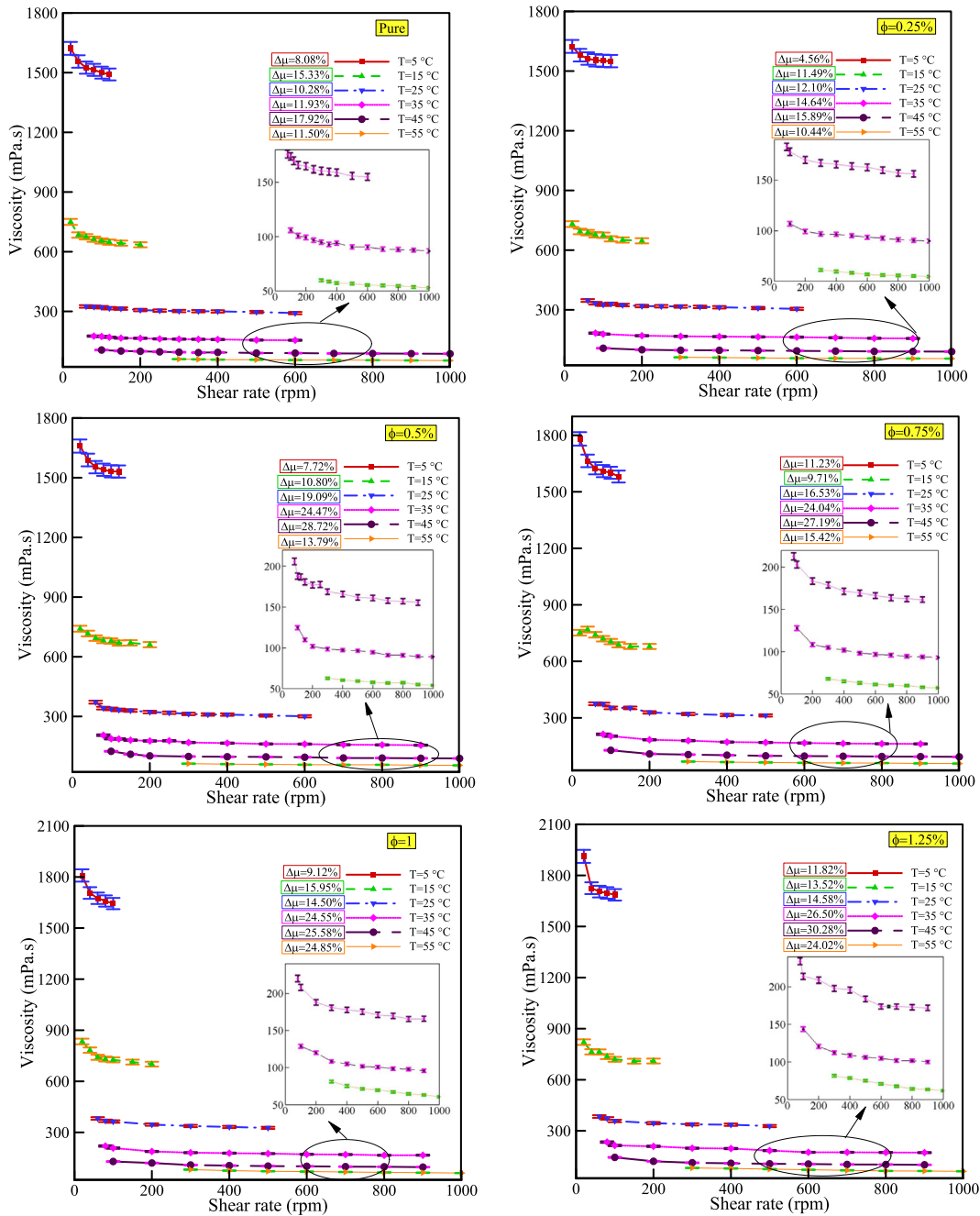


Fig. 5 Viscosity versus SR at different temperatures and VFs.

dependent and have nonlinear behavior. It is observed that Eqs (3) through (6) cannot accurately forecast the dynamic viscosity of the hybrid nanolubricant under investigation.

Hence, to correlate the studied hybrid nanofluid viscosity according to experiments, an innovative correlation (7) is established using curve fitting to predict the dynamic viscosity of CeO<sub>2</sub>-CuO/10W40 hybrid nanolubricant as a function of VF ( $0.25\% < \phi < 1.5\%$ ), temperature ( $5\text{ }^{\circ}\text{C} < T < 55\text{ }^{\circ}\text{C}$ ), and SR ( $20\text{ rpm} < \dot{\gamma} < 1000\text{ rpm}$ ) with a determination coefficient ( $R^2$ ) of 0.9916.

$$\begin{aligned}
 \mu_{nf} = & 2175.923 + 94.160\phi - 142.050T - 0.32589\dot{\gamma} + 137.015\phi^2 \\
 & + 3.5141T^2 + 0.0011366\dot{\gamma}^2 - 22.323\phi^3 - 0.030299T^3 \\
 & - 2.6648E - 7\dot{\gamma}^3 - 8.3412\phi T - 0.18571\phi\dot{\gamma} - 0.010491T\dot{\gamma} \\
 & - 2.7574\phi^2 T + 0.059742\phi^2\dot{\gamma} + 0.16275T^2\phi + 3.3810E - 04T^2\dot{\gamma} \\
 & + 7.8186E - 05\dot{\gamma}^2\phi - 1.7339E - 05\dot{\gamma}^2 T
 \end{aligned} \quad (7)$$

In addition to the curve fitting method, in this section, RSM-based statistical analysis is used to model the dynamic

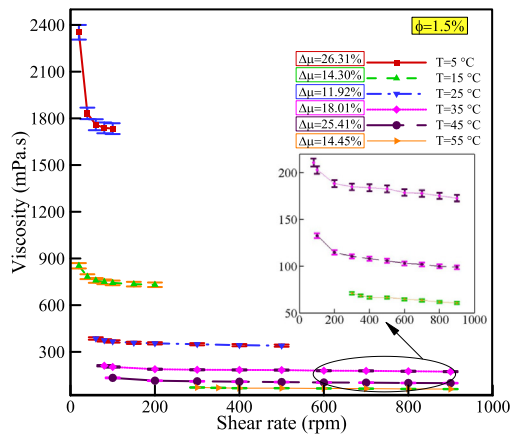


Fig. 5 (continued)

**Table 1** The minimum and maximum percentages of dynamic viscosity reduction with the SR.

		Minimum viscosity reduction (%)	Maximum viscosity reduction (%)
VF (%)	0 (10W40)	8.08	17.92
	0.25	4.56	15.89
	0.5	7.72	28.72
	0.75	11.23	27.19
	1	9.12	25.58
	1.25	11.82	30.28
	1.5	11.92	26.31
Temperature (°C)	5	4.56	26.31
	15	10.80	15.95
	25	10.28	19.09
	35	11.93	26.50
	45	15.89	30.28
	55	10.44	24.85

viscosity of CeO<sub>2</sub>-CuO/10W40 hybrid nanolubricant. Experimental data are employed as historical data for correlating the mathematical formula. Independent input variables include temperature, VF, and SR, and dynamic viscosity is taken into account as the dependent output variable. Tables 4 and 5 represent the input and response variable levels and characteristics, respectively.

Table 6 shows the statistical results of various functions. As it turns out, a linear function has the best-adjusted  $R^2$  and therefore is used as the optimal function.

The analysis of variance (ANOVA) for the anticipated model is summarized in Table 7. It is noteworthy that the linear model is used in this analysis. The  $F$ -value is 41200.00, and it shows that this model is authentic.

According to fit statistics in Table 8, the coefficient of  $R^2$  is equal to 0.9976 by using the linear function. Indeed, it shows the coincidence degree of the experimental data points and the model data. The adjusted  $R^2$  value is 0.9976, considering the effect of the equation's predicted constant coefficients. It highlights the conformity degree of the model data over the experimental data range. The predicted  $R^2$  value is 0.9975, which shows the predicted model data quality for data that do not fall within the experimental data range. Additionally, Adeq precision demonstrates that a signal-to-noise ratio higher than four is favorable (Peng et al., 2020). In this equation, the Adeq precision value is 597.5243, which shows a suitable signal.

The transform function for data normalization is set as  $y' = (y + k)^\lambda$  with  $k = 0$  and  $\lambda = -0.22$  as suggested by the software in the box-cox graphic illustrated in Fig. 10.

The regression diagram is shown in Fig. 11. As can be seen, an adequate consistency exists between the predicted model and the experimental data.

Fig. 12 shows the 3D surface diagrams of the model obtained via statistical analysis, where the effects of the temperature, VF, and SR on the response are shown.

The dynamic viscosity correlation derived from RSM is presented in Eq. (8).

$$\mu_{nf}^{-0.22} = \alpha_0 + \alpha_1\phi + \alpha_2T + \alpha_3\dot{\gamma} \quad (8)$$

where, the constants  $\alpha_0$ ,  $\alpha_1$ ,  $\alpha_2$ , and  $\alpha_3$  are + 0.181447, - 0.0077247, + 0.0038901, and 2.0326657E-5, respectively.

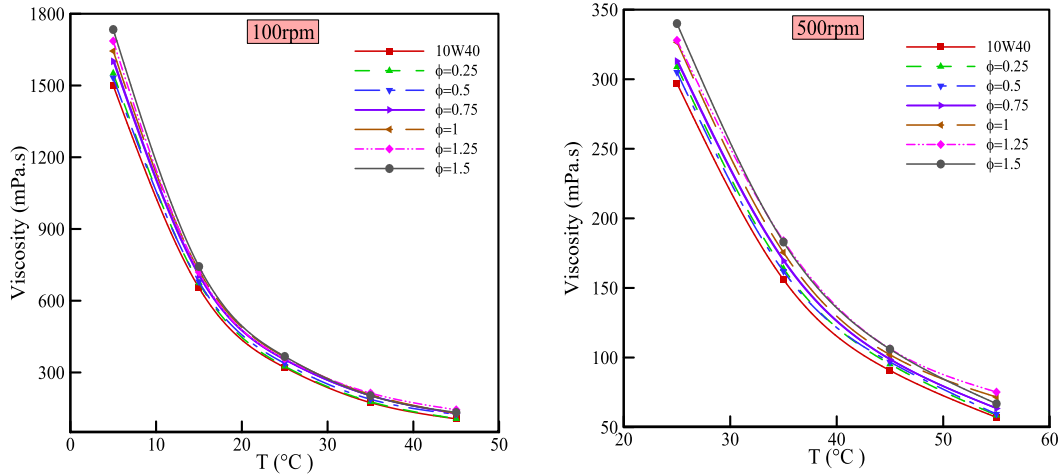
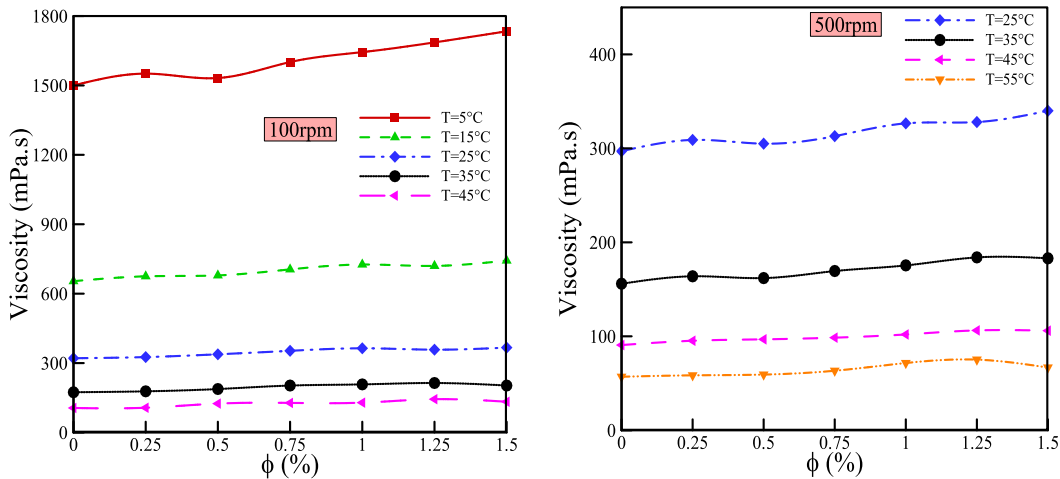
To ensure the accuracy of our presented correlations in Eqs. (7) and (8), the forecasted results by both of the developed correlations are compared with experimental data in Fig. 13. It can be found that the presented correlations predict the experimental data with relatively good accuracy. Since Eq. (8) is more straightforward than Eq. (7), it is recommended to use Eq. (8) to predict the dynamic viscosity of CeO<sub>2</sub>-CuO/10W40 hybrid nanolubricant. The proposed correlations in the present work can be applied to various applications, including numerical study (Shahsavari et al., 2018; Babu, 2022; Kavaya et al., 2022; Neethu et al., 2022; Shah et al., 2022; Bendrer et al., 2021; Ahmed, 2020; Naderi and Mohammadzadeh, 2020; Khorasanizadeh et al., 2017; Sepehrnia et al., 2019; Rahmati

**Table 2** Consistency index ( $m$ ) for hybrid nanolubricant.

Temperature (°C)	VF = 0% (10W40)	VF = 0.25%	VF = 0.5%	VF = 0.75%	VF = 1%	VF = 1.25%	VF = 1.5%
5	2.0924	1.872	2.1304	1.2155	2.4926	2.8584	6.3946
15	1.0719	0.09766	0.9833	1.0733	1.2477	1.1659	1.1892
25	0.4481	0.4609	0.5962	0.7013	0.6049	0.5978	0.5521
35	0.2696	0.2743	0.3951	0.45	0.4615	0.5392	0.3428
45	0.1917	0.1755	0.2892	0.3075	0.3467	0.4211	0.3158
55	0.01312	0.1342	0.1605	0.21	0.5308	0.6381	0.1881

**Table 3** Power law index ( $n$ ) for hybrid nanolubricant.

Temperature (°C)	VF = 0% (10W40)	VF = 0.25%	VF = 0.5%	VF = 0.75%	VF = 1%	VF = 1.25%	VF = 1.5%
5	0.9535	0.9737	0.954	0.9821	0.9413	0.9244	0.8121
15	0.932	0.9473	0.9487	0.9417	0.9253	0.935	0.9357
25	0.9527	0.9543	0.9229	0.9069	0.9298	0.9316	0.9444
35	0.9379	0.9407	0.8997	0.8805	0.8896	0.8777	0.9274
45	0.9167	0.9298	0.8746	0.8725	0.8625	0.845	0.8758
55	0.905	0.9056	0.887	0.854	0.7735	0.7551	0.8816

**Fig. 6** Viscosity changes versus temperature at various nanolubricant VFs.**Fig. 7** Viscosity changes versus VF at various nanolubricant temperatures.

et al., 2019), nano-lubricants (Afrand, 2016; Esfe et al., 2022; Arif et al., 2021; Khan et al., 2019), microchannel heat sinks (Sepehrnia et al., 2021; Khorasanizadeh and Sepehrnia, 2017; Khorasanizadeh and Sepehrnia, 2018; Khorasanizadeh and Sepehrnia, 2016; Khorasanizadeh et al., 2019;

Khorasanizadeh and Sepehrnia, 2018; Sepehrnia et al., 2018; Sepehrnia et al., 2019), heat exchangers (Shahsavari et al., 2019; Alazwari and Safaei, 2021; Davoudi et al., 2021), and automotive industry (Jamil and Ali, 2020; Abbas, 2020; Arif et al., 2022).

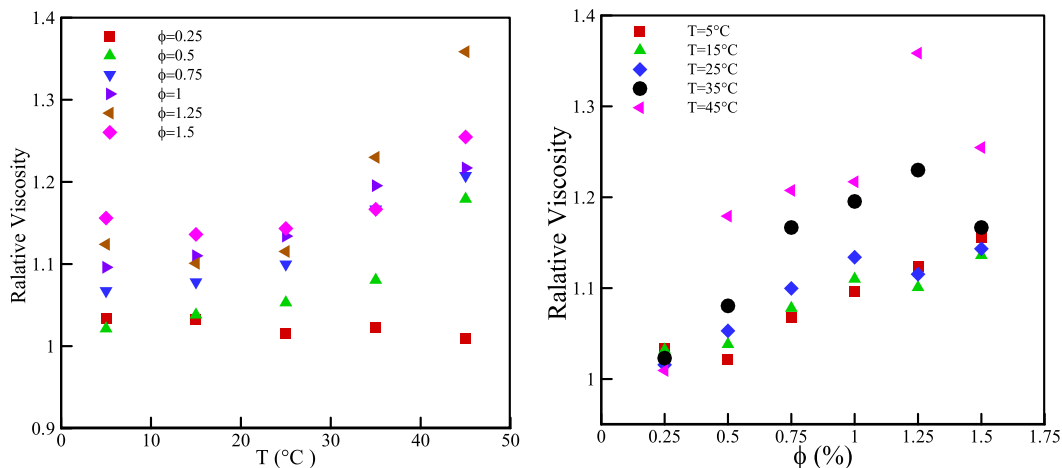


**Fig. 8** Relative viscosity changes versus temperature and VF for SR of 100 rpm.

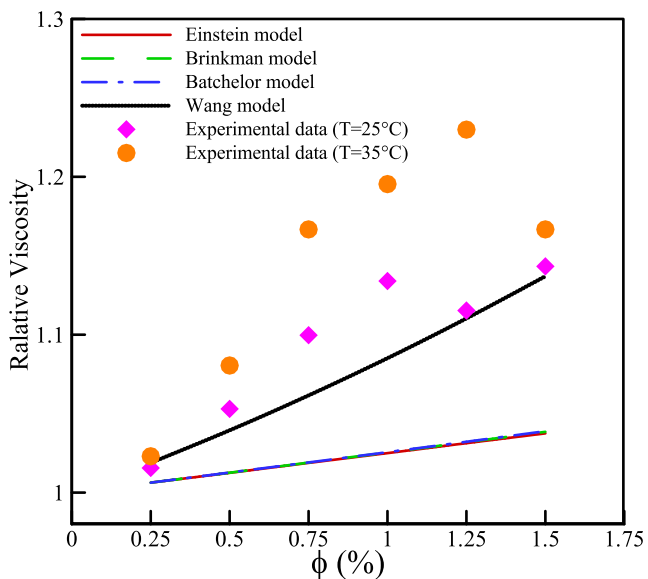


**Fig. 9**  $\mu_r$  versus VF at SR of 100 rpm using various models.

**Table 6** Statistical Results of Different Functions.

Source	Sequential p-value	Adjusted R <sup>2</sup>	Predicted R <sup>2</sup>	
Linear	< 0.0001	0.9976	0.9975	Suggested
2FI	< 0.0001	0.9978	0.9978	
Quadratic	< 0.0001	0.9984	0.9983	
Cubic	< 0.0001	0.9991	0.9990	
Quartic	< 0.0001	0.9995	0.9993	
Fifth	< 0.0001	0.9996	0.9995	
Sixth	< 0.0001	0.9997	0.9995	

### 3.5. Sensitivity analysis

Sensitivity analysis is used to determine the sensitivity of dynamic viscosity of the CeO<sub>2</sub>-CuO/10W40 hybrid nanolubricant to varying nanofluid VF. For this purpose, Eq. (9) is used.

$$\mu_{nf} \text{ Sensitivity}(\%) = \left( \frac{\mu_{nf,Afterchange} - \mu_{nf,Basecondition}}{\mu_{nf,Basecondition}} \right) \times 100 \quad (9)$$

**Table 4** Input variables of the RSM model.

Factor	Name	Units	Type	SubType	Minimum	Maximum	Coded Low	Coded High	Mean	Std. Dev.
A	VF	%	Numeric	Continuous	0.250	1.50	-1 ↔ 0.25	+1 ↔ 1.50	0.8460	0.4302
B	T	°C	Numeric	Continuous	5.0	55.00	-1 ↔ 5.0	+1 ↔ 55.00	32.12	15.89
C	SR	rpm	Numeric	Continuous	20.0	1000.00	-1 ↔ 20.0	+1 ↔ 1000.00	361.59	294.42

**Table 5** Characteristic of the RSM model response.

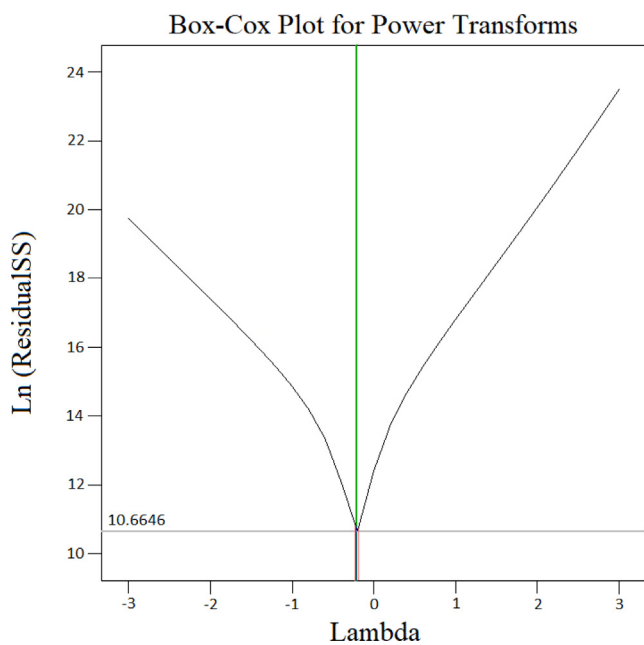
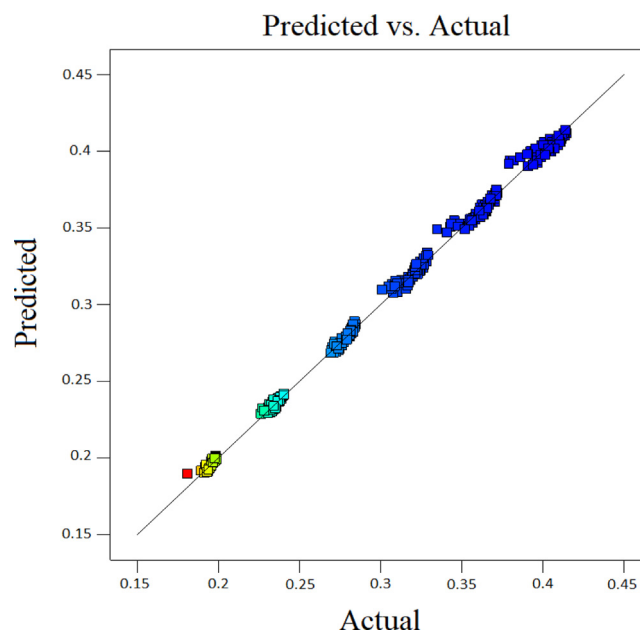
Response	Name	Units	Observations	Minimum	Maximum	Mean	Std. Dev.	Ratio	Transform	Model
R1	Dynamic viscosity	mPa.s	302.00	54.4	2353	418.84	492.96	43.25	Power	Linear

**Table 7** Analysis of variance for the linear model.

Source	Sum of Squares	df	Mean Square	F-value	p-value	
Model	1.31	3	0.4375	41200.00	< 0.0001	significant
A-phi	0.0033	1	0.0033	312.56	< 0.0001	
B-T	0.6074	1	0.6074	57209.40	< 0.0001	
C-S R	0.0057	1	0.0057	536.94	< 0.0001	
Residual	0.0032	298	0.0000			
Cor Total	1.32	301				

**Table 8** Fit statistics.

Std. Dev.	0.0033	$R^2$	0.9976
Mean	0.3072	Adjusted $R^2$	0.9976
C.V. %	1.06	Predicted $R^2$	0.9975
		Adeq Precision	597.5243

**Fig. 10** The box-cox plot for determination of the modified transform function.**Fig. 11** Regression diagram of the predicted values with experimental data.

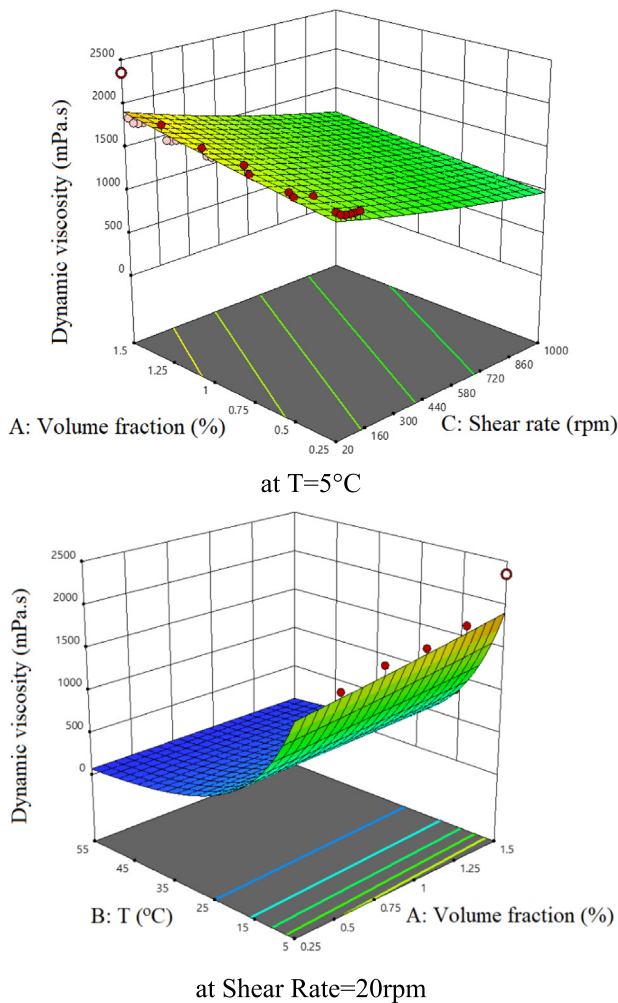


**Fig. 12** Model output diagrams by RSM: (a) interaction within SR and VF on dynamic viscosity; (b) interaction within temperature and VF on dynamic viscosity.

The  $\mu_{nf}$  sensitivity to the hybrid nanofluid VF is represented in Fig. 14. It can be found that the  $\mu_{nf}$  sensitivity increases with increasing nanofluid VF, taking into account a constant SR of 100 rpm. According to Fig. 14, The  $\mu_{nf}$  sensitivity to temperature and VF is generally low (below 3%). The highest viscosity sensitivity occurs for the VF = 1.25% at a temperature of 55 °C, which is equal to -2.84%.

**4. Conclusion**

In the present work, the measurement of dynamic viscosity of CeO<sub>2</sub>-CuO/10W40 hybrid nanolubricant is experimentally accomplished at various VFs (0.25% <  $\phi$  < 1.5%), temperatures (5 °C < T < 55 °C) and SRs (20 rpm <  $\dot{\gamma}$  < 1000 rpm). The main results of this study are as follows:

1. 10W40 engine oil behaves non-Newtonian, so that with increasing SR, its dynamic viscosity decreases between 8.08% and 17.92%, and the maximum reduction in dynamic viscosity corresponds to a temperature of 45 °C.
2. The CeO<sub>2</sub>-CuO/10W40 hybrid nano-lubricant has a non-Newtonian behavior in all VFs, so that with increasing SR, its dynamic

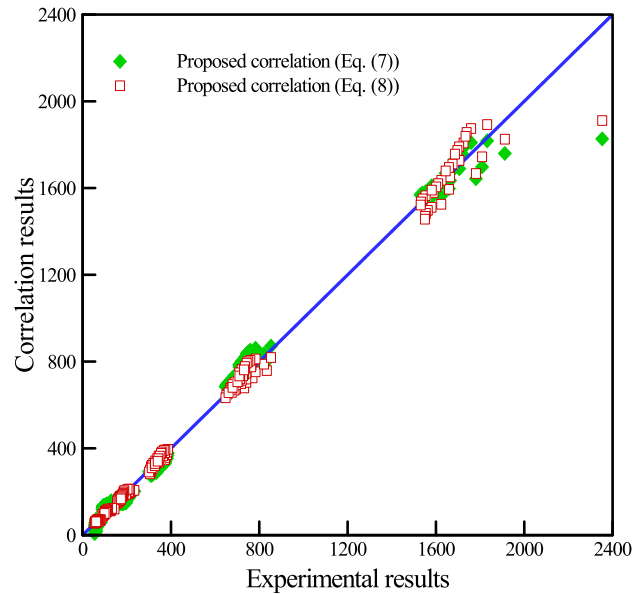


**Fig. 13** Comparing the measured viscosity with developed correlations.

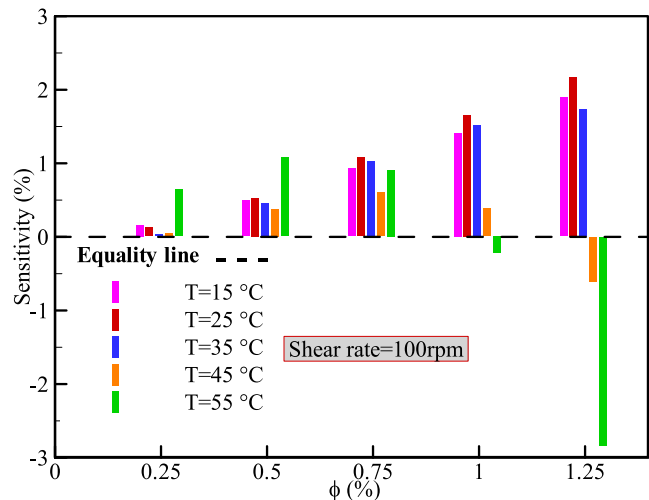


**Fig. 14** Sensitivity analysis diagram for the CeO<sub>2</sub>-CuO/10W40 hybrid nano-lubricant.

viscosity decreases between 4.56% and 30.28%, which the most significant reduction in dynamic viscosity occurs at VF of 1.25% and temperature of 45 °C.

3. Two three-variable functional relationships are established to precisely evaluate the dynamic viscosity of CeO<sub>2</sub>-CuO/10W40 hybrid nanolubricant at different VFs, SRs, and temperatures.

4. The relation obtained from the RSM method is more straightforward than the relation obtained from the curve fitting method and its accuracy is slightly higher, so it is recommended to use it to predict the dynamic viscosity of CeO<sub>2</sub>-CuO/10W40 hybrid nanolubricant.

5. Based on sensitivity analysis, the  $\mu_{nf}$  sensitivity increases with increasing nanofluid VF, and  $\mu_{nf}$  is more sensitive to temperature changes than volume fraction.

## Declaration of Competing Interest

The authors declare that they have no known competing financial interests or personal relationships that could have appeared to influence the work reported in this paper.

## References

- Abbas, F. et al, 2020. Nanofluid: potential evaluation in automotive radiator. *J. Mol. Liq.* 297, 112014.
- Afrand, M. et al, 2016. Prediction of dynamic viscosity of a hybrid nano-lubricant by an optimal artificial neural network. *Int. Commun. Heat Mass Transfer* 76, 209–214.
- Afrand, M., Nadooshan, A.A., Hassani, M., Yarmand, H., Dahari, M., 2016. Predicting the viscosity of multi-walled carbon nanotubes/water nanofluid by developing an optimal artificial neural network based on experimental data. *Int. Commun. Heat Mass Transfer* 77, 49–53.
- Aghaei, A., Khorasanizadeh, H., Sheikhzadeh, G.A., 2018. Measurement of the dynamic viscosity of hybrid engine oil-Cuo-MWCNT nanofluid, development of a practical viscosity correlation and utilizing the artificial neural network. *Heat Mass Transf.* 54 (1), 151–161.
- Ahmed, S.E., 2020. Caputo fractional convective flow in an inclined wavy vented cavity filled with a porous medium using Al<sub>2</sub>O<sub>3</sub>-Cu hybrid nanofluids. *Int. Commun. Heat Mass Transfer* 116, 104690.
- Alazwari, M.A., Safaei, M.R., 2021. Combination effect of baffle arrangement and hybrid nanofluid on thermal performance of a shell and tube heat exchanger using 3-D homogeneous mixture model. *Mathematics* 9 (8), 881.
- Arif, M., Kumam, P., Khan, D., Watthayu, W., 2021. Thermal performance of GO-MoS<sub>2</sub>/engine oil as Maxwell hybrid nanofluid flow with heat transfer in oscillating vertical cylinder. *Case Stud. Therm. Eng.* 27, 101290.
- Arif, M., Kumam, P., Kumam, W., Mostafa, Z., 2022. Heat transfer analysis of radiator using different shaped nanoparticles water-based ternary hybrid nanofluid with applications: a fractional model. *Case Stud. Therm. Eng.* 31, 101837.
- Asadi, A., Asadi, M., Rezaei, M., Siahmargoi, M., Asadi, F., 2016. The effect of temperature and solid concentration on dynamic viscosity of MWCNT/MgO (20–80)–SAE50 hybrid nano-lubricant and proposing a new correlation: an experimental study. *Int. Commun. Heat Mass Transfer* 78, 48–53.
- Asadi, A., Alarifi, I.M., Nguyen, H.M., Moayedi, H., 2021. Feasibility of least-square support vector machine in predicting the effects of shear rate on the rheological properties and pumping power of MWCNT–MgO/oil hybrid nanofluid based on experimental data. *J. Therm. Anal. Calorim.* 143 (2), 1439–1454.
- Asadi, M., Asadi, A., 2016. Dynamic viscosity of MWCNT/ZnO–engine oil hybrid nanofluid: an experimental investigation and new correlation in different temperatures and solid concentrations. *Int. Commun. Heat Mass Transfer* 76, 41–45.
- Asadi, A., Bakhtiyari, A.N., Alarifi, I.M., 2021. Predictability evaluation of support vector regression methods for thermophysical properties, heat transfer performance, and pumping power estimation of MWCNT/ZnO–engine oil hybrid nanofluid. *Eng. Comput.* 37 (4), 3813–3823.
- Babu, M.J. et al, 2022. Squeezed flow of polyethylene glycol and water based hybrid nanofluid over a magnetized sensor surface: a statistical approach. *Int. Commun. Heat Mass Transfer* 135, 106136.
- Barkhordar, A., Ghasemiasl, R., Armaghani, T., 2021. Statistical study and a complete overview of nanofluid viscosity correlations: a new look. *J. Therm. Anal. Calorim.* 1–34
- Batchelor, G., 1977. The effect of Brownian motion on the bulk stress in a suspension of spherical particles. *J. Fluid Mech.* 83 (1), 97–117.
- Bendrer, B., Abderrahmane, A., Ahmed, S.E., Raizah, Z.A., 2021. 3D magnetic buoyancy-driven flow of hybrid nanofluids confined wavy cubic enclosures including multi-layers and heated obstacle. *Int. Commun. Heat Mass Transfer* 126, 105431.
- H. C. Brinkman, “The viscosity of concentrated suspensions and solutions,” *The Journal of chemical physics*, vol. 20, no. 4, pp. 571–571, 1952.
- Cao, Y., Khan, A., Abdi, A., Ghadiri, M., 2021. Combination of RSM and NSGA-II algorithm for optimization and prediction of thermal conductivity and viscosity of bioglycol/water mixture containing SiO<sub>2</sub> nanoparticles. *Arab. J. Chem.* 14, (7) 103204.
- Dalkılıç, A.S. et al, 2018. Experimental investigation on the viscosity characteristics of water based SiO<sub>2</sub>-graphite hybrid nanofluids. *Int. Commun. Heat Mass Transfer* 97, 30–38.
- Davoudi, A., Daneshmand, S., Monfared, V., Mohammadzadeh, K., 2021. Numerical simulation on heat transfer of nanofluid in conical spiral heat exchanger. *Prog. Comput. Fluid Dyn., Int. J.* 21 (1), 52–63.
- Einstein, A., 1911. Berichtigung zu meiner arbeit: Eine neue bestimmung der moleküldimensionen. *Ann. Phys.* 339 (3), 591–592.
- Esfé, M.H., Arani, A.A.A., Rezaie, M., Yan, W.-M., Karimipour, A., 2015. Experimental determination of thermal conductivity and dynamic viscosity of Ag–MgO/water hybrid nanofluid. *Int. Commun. Heat Mass Transfer* 66, 189–195.
- Esfé, M.H., Zabihi, F., Rostamian, H., Esfandeh, S., 2018. Experimental investigation and model development of the non-Newtonian behavior of CuO-MWCNT-10w40 hybrid nano-lubricant for lubrication purposes. *J. Mol. Liq.* 249, 677–687.
- Esfé, M.H., Dalir, R., Bakhtiari, R., Afrand, M., 2019. Simultaneous effects of multi-walled carbon nanotubes and copper oxide nanoparticles on the rheological behavior of cooling oil: application for refrigeration systems. *Int. J. Refrig.* 104, 123–133.
- Esfé, M.H., Saedodin, S., Toghraie, D., 2022. Experimental study and modeling the SiO<sub>2</sub>-MWCNT (30: 70)/SAE40 hybrid nano-lubricant flow based on the response surface method to identify the optimal lubrication conditions. *Int. Commun. Heat Mass Transfer* 130, 105771.
- Esfé, M.H., Kiannejad, M., Esfandeh, S., Emami, M.R.S., Toghraie, D., 2022. Influence of different parameters on the rheological behavior MWCNT (30%)-TiO<sub>2</sub> (70%)/SAE50 hybrid nano-lubricant using of Response Surface Methodology and Artificial Neural Network methods. *Arab. J. Chem.* 104285
- Esfé, M.H., Kamyab, M.H., Ardeshiri, E.M., Toghraie, D., 2023. Study of MWCNT (40%)–CuO (60%)/10W40 hybrid nanofluid for improving laboratory oil performance by laboratory method and statistical response surface methodology. *Alex. Eng. J.* 63, 115–125.
- Ghaffarkhah, A., Bazzi, A., Dijejin, Z.A., Talebkeikhah, M., Moraveji, M.K., Agin, F., 2019. Experimental and numerical analysis of rheological characterization of hybrid nano-lubricants containing COOH-Functionalized MWCNTs and oxide nanoparticles. *Int. Commun. Heat Mass Transfer* 101, 103–115.
- Giwa, S., Sharifpur, M., Goodarzi, M., Alsulami, H., Meyer, J., 2021. Influence of base fluid, temperature, and concentration on the thermophysical properties of hybrid nanofluids of alumina–ferrofluid: experimental data, modeling through enhanced ANN, ANFIS, and curve fitting. *J. Therm. Anal. Calorim.* 143 (6), 4149–4167.
- Huminić, G., Huminić, A., 2018. Hybrid nanofluids for heat transfer applications—a state-of-the-art review. *Int. J. Heat Mass Transf.* 125, 82–103.
- Jamil, F., Ali, H.M., 2020. Applications of hybrid nanofluids in different fields. In: *Hybrid nanofluids for convection heat transfer*. Elsevier, pp. 215–254.
- Kavya, S., Nagendramma, V., Ahammad, N.A., Ahmad, S., Raju, C., Shah, N.A., 2022. Magnetic-hybrid nanoparticles with stretching/shrinking cylinder in a suspension of MoS<sub>4</sub> and copper nanoparticles. *Int. Commun. Heat Mass Transfer* 136, 106150.

- Khan, I., Saeed, K., Khan, I., 2019. Nanoparticles: properties, applications and toxicities. *Arab. J. Chem.* 12 (7), 908–931.
- H. Khorasanizadeh and M. Sepehrnia, “Thermal performance and entropy generation analysis of nanofluid flow in a trapezoidal heat sink with different arrangements,” *Amirkabir Journal of Mechanical Engineering*, 2018.
- Khorasanizadeh, H., Sepehrnia, M., 2016. Effects of different inlet/outlet arrangements on performance of a trapezoidal porous microchannel heat sink. *Modares Mech. Eng.* 16 (8), 269–280.
- Khorasanizadeh, H., Sepehrnia, M., 2017. Performance evaluation of a trapezoidal microchannel heat sink with various entry/exit configurations utilizing variable properties. *J. Appl. Fluid Mech.* 10 (6), 1547–1559.
- Khorasanizadeh, H., Sepehrnia, M., 2018. Three dimensional numerical study on a trapezoidal microchannel heat sink with different inlet/outlet arrangements utilizing variable properties nanofluid. *Transp. Phenom. Nano Micro Scales* 6 (2), 133–151.
- Khorasanizadeh, H., Sepehrnia, M., Sadeghi, R., 2017. Three dimensional investigations of inlet/outlet arrangements and nanofluid utilization effects on a triangular microchannel heat sink performance. *Modares Mech. Eng.* 16 (12), 27–38.
- Khorasanizadeh, H., Sepehrnia, M., Sadeghi, R., 2019. Investigation of nanofluid flow field and conjugate heat transfer in a MCHS with four different arrangements. *Amirkabir J. Mech. Eng.* 51 (2), 113–116.
- Mansourian, R., Mousavi, S.M., Michaelides, E.E., 2021. Improving the thermo-physical and rheological properties of crude oil (CO) by the synthesized CuO/SiO<sub>2</sub>/CaP nanocomposite for drag reduction through horizontal pipelines. *Appl. Nanosci.* 11, 347–362.
- Moghaddam, M.A., Motahari, K., 2017. Experimental investigation, sensitivity analysis and modeling of rheological behavior of MWCNT-CuO (30–70)/SAE40 hybrid nano-lubricant. *Appl. Therm. Eng.* 123, 1419–1433.
- Mokarian, M., Ameri, E., 2022. The effect of Mg(OH)<sub>2</sub> nanoparticles on the rheological behavior of base engine oil SN500 HVI and providing a predictive new correlation of nanofluid viscosity. *Arab. J. Chem.* 15, (6) 103767.
- Naderi, B., Mohammadzadeh, K., 2020. Numerical unsteady simulation of nanofluid flow over a heated angular oscillating circular cylinder. *J. Therm. Anal. Calorim.* 139 (1), 721–739.
- Neethu, T., Sabu, A., Mathew, A., Wakif, A., Areekara, S., 2022. Multiple linear regression on bioconvective MHD hybrid nanofluid flow past an exponential stretching sheet with radiation and dissipation effects. *Int. Commun. Heat Mass Transfer* 135, 106115.
- Peng, Y., Khaled, U., Al-Rashed, A.A., Meer, R., Goodarzi, M., Sarafraz, M., 2020. Potential application of Response Surface Methodology (RSM) for the prediction and optimization of thermal conductivity of aqueous CuO (II) nanofluid: a statistical approach and experimental validation. *Physica A* 554, 124353.
- Rahmati, A.R., Sepehrnia, M., Motamedian, M., 2019. “Numerical simulation of turbulent natural convection of nanofluid with thermal radiation inside a tall enclosure under the influence of magnetohydrodynamic”. *Heat Transfer—Asian Res.* 48 (2), 520–538.
- Sajeeb, A., Rajendrakumar, P.K., 2019. Investigation on the rheological behavior of coconut oil based hybrid CeO<sub>2</sub>/CuO nanolubricants. *Proc. Inst. Mech. Eng., Part J: J. Eng. Tribol.* 233 (1), 170–177.
- Sajeeb, A., Rajendrakumar, P.K., 2020. Tribological assessment of vegetable oil based CeO<sub>2</sub>/CuO hybrid nano-lubricant. *Proc. Inst. Mech. Eng., Part J: J. Eng. Tribol.* 234 (12), 1940–1956.
- M. Sepehrnia, G. Abaei, Z. Khosromirza, and F. RooghaniYazdi, “Numerical Simulation and Designing Artificial Neural Network for Water-Diamond Nanofluid Flow for Micro-Scale Cooling of Medical Equipment,” in *2018 25th National and 3rd International Iranian Conference on Biomedical Engineering (ICBME)*, 2018: IEEE, pp. 1–6.
- M. Sepehrnia, H. Khorasanizadeh, and M. B. Shafii, “Numerical simulation of magnetic field effect on thermal and thermo-hydraulic performance and entropy generation of a silicon microchannel heat sink under uniform heat flux,” *Amirkabir Journal of Mechanical Engineering*, 2019.
- Sepehrnia, M., Sheikhzadeh, G., Abaei, G., Motamedian, M., 2019. “Study of flow field, heat transfer, and entropy generation of nanofluid turbulent natural convection in an enclosure utilizing the computational fluid dynamics-artificial neural network hybrid method”. *Heat Transfer—Asian Res.* 48 (4), 1151–1179.
- Sepehrnia, M., Khorasanizadeh, H., Shafii, M.B., 2021. Effect of transverse and parallel magnetic fields on thermal and thermo-hydraulic performances of ferro-nanofluid flow in trapezoidal microchannel heat sink. *Int. J. Numer. Meth. Heat Fluid Flow.*
- Sepehrnia, M., Mohammadzadeh, K., Veyseh, M.M., Agah, E., Amani, M., 2022. Rheological behavior of engine oil based hybrid nanofluid containing MWCNT and ZnO nanopowders: experimental analysis, developing a novel correlation and neural network modeling. *Powder Technol.* 117492
- Sepehrnia, M., Maleki, H., Karimi, M., Nabati, E., 2022. Examining rheological behavior of CeO<sub>2</sub>-GO-SA/10W40 ternary hybrid nanofluid based on experiments and COMBI/ANN/RSM modeling. *Sci. Rep.* 12 (1), 1–22.
- Sepehrnia, M., Lotfalipour, M., Malekiyan, M., Karimi, M., Farahani, S.D., 2022. Rheological behavior of SAE50 Oil-SnO<sub>2</sub>-CeO<sub>2</sub> hybrid nanofluid: experimental investigation and modeling utilizing response surface method and machine learning techniques. *Nanoscale Res. Lett.* 17 (1), 1–22.
- Shah, N.A., Wakif, A., El-Zahar, E.R., Thumma, T., Yook, S.-J., 2022. Heat transfers thermodynamic activity of a second-grade ternary nanofluid flow over a vertical plate with Atangana-Baleanu time-fractional integral. *Alex. Eng. J.* 61 (12), 10045–10053.
- Shahsavari, A., Ansarian, R., Bahiraei, M., 2018. Effect of line dipole magnetic field on entropy generation of Mn-Zn ferrite ferrofluid flowing through a minichannel using two-phase mixture model. *Powder Technol.* 340, 370–379.
- Shahsavari, A., Rahimi, Z., Salehipour, H., 2019. Nanoparticle shape effects on thermal-hydraulic performance of boehmite alumina nanofluid in a horizontal double-pipe minichannel heat exchanger. *Heat Mass Transf.* 55 (6), 1741–1751.
- Wang, X.-Q., Mujumdar, A.S., 2007. Heat transfer characteristics of nanofluids: a review. *Int. J. Therm. Sci.* 46 (1), 1–19.